Molecular Biology of the Cell
Vol. 7, 595–611, April 1996

Construction and Characterization of Secreted and Chimeric Transmembrane Forms of *Drosophila* Acetylcholinesterase: A Large Truncation of the C-Terminal Signal Peptide Does Not Eliminate Glycoinositol Phospholipid Anchoring

John P. Incardona* and Terrone L. Rosenberry†‡

*Department of Genetics and †Department of Pharmacology, School of Medicine, Case Western Reserve University, Cleveland, Ohio 44106

Submitted June 28, 1995; Accepted January 24, 1996
Monitoring Editor: Keith R. Yamamoto

Despite advances in understanding the cell biology of glycoinositol phospholipid (GPI)-anchored proteins in cultured cells, the in vivo functions of GPI anchors have remained elusive. We have focused on *Drosophila* acetylcholinesterase (AChE) as a model GPI-anchored protein that can be manipulated in vivo with sophisticated genetic techniques. In *Drosophila*, AChE is found only as a GPI-anchored G_2 form encoded by the *Ace* locus on the third chromosome. To pursue our goal of replacing wild-type GPI-anchored AChE with forms that have alternative anchor structures in transgenic flies, we report here the construction of two secreted forms of *Drosophila* AChE (SEC1 and SEC2) and a chimeric form (TM-AChE) anchored by the transmembrane and cytoplasmic domains of herpes simplex virus type 1 glycoprotein C. To confirm that the biochemical properties of these AChEs were unchanged from GPI-AChE except as predicted, we made stably transfected *Drosophila* Schneider Line 2 (S2) cells expressing each of the four forms. TM-AChE, SEC1, and SEC2 had the same catalytic activity and quaternary structure as wild type. TM-AChE was expressed as an amphiphilic membrane-bound protein resistant to an enzyme that cleaves GPI-AChE (phosphatidylinositol-specific phospholipase C), and the same percentage of TM-AChE and GPI-AChE was on the cell surface according to immunofluorescence and pharmacological data. SEC1 and SEC2 were constructed by truncating the C-terminal signal peptide initially present in GPI-AChE: in SEC1 the last 25 residues of this 34-residue peptide were deleted while in SEC2 the last 29 were deleted. Both SEC1 and SEC2 were efficiently secreted and are very stable in culture medium; with one cloned SEC1-expressing line, AChE accumulated to as high as 100 mg/liter. Surprisingly, 5–10% of SEC1 was attached to a GPI anchor, but SEC2 showed no GPI anchoring. Since no differences in catalytic activity were observed among the four AChEs, and since the same percentage of GPI-AChE and TM-AChE were on the cell surface, we contend that in vivo experiments in which GPI-AChE is replaced can be interpreted solely on the basis of the altered anchoring domain.

INTRODUCTION

The covalent modification of cell surface proteins by glycoinositol phospholipids (GPIs)[1] is a general mechanism by which cells from a large variety of eukaryotic organisms anchor certain proteins on the outer surface of the plasma membrane. Although biochemical studies have elucidated the detailed structures of GPI anchors and their biosynthetic pathways (Englund, 1993), the functional roles of GPI anchors have remained elusive. Since GPI oligosaccharide core stru-

‡ Corresponding author: Department of Pharmacology, Case Western Reserve University School of Medicine, Cleveland, OH 44106-4965.

[1] Abbreviations used: AChE, acetylcholinesterase; DTT, dithiothreitol; endo H, endoglycosidase H; ETP, echothiophate; GPI, glycoinositol phospholipid; HSV-1 gC, herpes simplex virus

cures are highly conserved from protozoans to mammals and because many proteins have both GPI-anchored and transmembrane forms, it seems likely that GPIs have functions in addition to simply anchoring proteins on cell surfaces. An early hypothesis was that GPI-anchoring could be a means of regulating cell surface expression of a protein through GPI-specific phospholipases. GPI-specific phospholipases C and D have been isolated from *Trypanosoma brucei* (Herald *et al.*, 1986), and mammalian liver (Fox *et al.*, 1987), serum (Low and Prasad, 1988; Davitz *et al.*, 1989), and brain (Hoener *et al.*, 1990), respectively, but no physiological function has been attributed to these enzymes. Studies of the cell biology of GPI-anchored proteins have shown that a GPI acts as an apical, and possibly axonal, sorting signal in polarized epithelial cells and some mammalian neurons, respectively (Lisanti *et al.*, 1989; Dotti *et al.*, 1991). Furthermore, GPIs appear to associate with glycosphingolipids and cholesterol in membrane microdomains during transport to the apical surface of Madin-Darby canine kidney cells (Brown and Rose, 1992). These microdomains can be isolated biochemically as cold Triton X-100–insoluble complexes that may be equivalent to caveolae (Anderson, 1993; Sargiacomo *et al.*, 1993); related complexes are also derived from the *trans*-Golgi network (Dupree *et al.*, 1993). Several lines of evidence suggest that some GPI-anchored proteins can transduce an extracellular signal and may interact with *src*-family tyrosine kinases by an undetermined mechanism. Cross-linking of GPI-anchored T cell antigens by antibody leads to T cell activation (reviewed by Robinson, 1991), and GPI-anchored proteins and other glycolipids co-immunoprecipitate with *lck* and *fyn* tyrosine kinases in several mammalian lymphocyte lines (Štefanová *et al.*, 1991; Cinek and Hořječí, 1992; Thomas and Samelson, 1992).

Although many studies have modified transmembrane or secreted proteins with a GPI anchor and observed the effects on protein sorting, few studies have done the reverse: convert a normally GPI-anchored protein to a transmembrane form and assess the effect on the function of the protein. The GPI-anchored class I MHC antigen Qa-2 has been converted to a chimeric transmembrane form that was unable to initiate T cell activation upon cross-linking by antibody (Robinson *et al.*, 1989). However, as the normal function of Qa-2 remains to be determined, this manipulation does not provide a satisfying answer to the question of the physiological role of GPI-anchoring.

(Abbrev. cont.) type 1 glycoprotein C; MSF, methanesulfonyl fluoride; ND-PAGE, nondenaturing polyacrylamide gel electrophoresis; PBS, phosphate-buffered saline; PIPLC, phosphatidylinositol-specific phospholipase C; TM, transmembrane; VSV G, vesicular stomatitis virus glycoprotein.

The central questions thus remain: What is the functional difference between anchoring by a GPI or a conventional transmembrane peptide, and how does the GPI contribute to the physiological roles of the proteins that bear it? To address these questions with a protein whose function is well characterized and can be studied in vivo, we have focused on *Drosophila* acetylcholinesterase (AChE). AChE hydrolyzes acetylcholine to terminate synaptic transmission at cholinergic synapses. In *Drosophila* there is a single form of AChE, a disulfide-linked dimer of GPI-anchored catalytic subunits, encoded by the *Ace* locus at 87E2–4 on the third chromosome. Acetylcholine is the major excitatory transmitter in the insect central nervous system; AChE is thus widely expressed in the *Drosophila* central nervous system but largely excluded from the periphery. The enzyme is extremely well characterized in terms of both classical and molecular genetics and in its biochemical properties (reviewed by Restifo and White, 1990). In this paper we describe the construction, cell culture expression, and biochemical characterization of two classes of *Drosophila* AChE in which the GPI has been replaced. One is secreted and the other is attached to the cell surface by the transmembrane domain of human herpes simplex virus type 1 glycoprotein C (HSV-1 gC). These AChE constructs also have been introduced into transgenic flies devoid of wild-type AChE (Incardona and Rosenberry, 1996).

MATERIALS AND METHODS

Plasmids and Vectors

pE18 contains a full length *Ace* cDNA subclone in pBluescript; most of the 5′-untranslated region has been deleted to remove several false initiation codons (Hall and Spierer, 1986). pAR-CT3 contains the cDNA for a truncation of vesicular stomatitis virus glycoprotein (VSV G) lacking the cytoplasmic domain (Crise *et al.*, 1989). The coding sequence for HSV-1 gC was obtained from pTZ18R-gC (a gift from T. Holland, Wayne State University, Detroit, MI). Expression vector pP_{ac} has been used in a variety of *Drosophila* cell lines; constitutive expression is driven by the promoter from the *Drosophila actin 5C* locus (Krasnow *et al.*, 1989). The coding sequence for hygromycin B phosphotransferase was obtained from pLG89 (Gritz and Davies, 1983).

Construction of AChEs with Altered Anchor Domains

To produce secreted forms of AChE, the *Ace* C-terminal sequence extending through codon 649 and containing the GPI addition signal was truncated. pSEC1 was constructed utilizing the *Xmn*I site between codons 621 and 622. An *Nhe*I linker of sequence CTAGCTAGCTAG (New England Biolabs, Beverly, MA) was ligated into a linearized partial *Xmn*I digest of pE18 to generate pSEC1 (Figure 1A). pSEC2 was produced as outlined in Figure 1B. The transmembrane domain of HSV-1 gC was obtained from pTZ18R-gC by isolating a 181-bp *Pvu*I/*Hin*PI fragment after blunting both ends with T4 DNA polymerase. When this fragment is ligated into the filled-in *Nhe*I site of pSEC1, the transmembrane domain is in frame and the Ile^{476} codon of HSV-1 gC is converted to Ser^{624} of TM-AChE. The new C-terminal sequence (Figure 1C) is

terminated by the HSV-1 gC stop codon. A transmembrane construct was built with a similar strategy utilizing the transmembrane domain of VSV G glycoprotein. A truncated form of VSV G bearing only three residues of the cytoplasmic domain was obtained from the plasmid pAR-CT3 as a 216-bp *AluI*/*StuI* fragment and cloned into pSEC1 cut with *NheI* and blunted with Klenow. All mutant constructs were confirmed by sequencing with the Sanger dideoxy chain termination method utilizing double-stranded miniprep DNA and Sequenase 2.0. Prediction of RNA secondary structures for the SEC1 3′ end was performed using the Mulfold program (Jaeger *et al.*, 1989).

Transfection of Schneider Line 2 Cells and Selection of Stable Lines

All AChE cDNA constructs were removed as 3.3-kb fragments from the corresponding pBluescript vectors with *Asp*718 (Figure 1A) and cloned into pP_{ac} after modifying its *Bam*HI site with an *Asp*718 linker. The coding sequence for hygromycin B phosphotransferase (*hph*) was obtained as a 1-kb *Bam*HI fragment from pLG89 and cloned into pP_{ac} to generate pP_{ac}Hph. Schneider Line 2 (S2) cells were cultured at 25°C in tightly capped 75 cm^2 T-flasks in complete medium consisting of 4 volumes stock M3 medium (Shields and Sang, 1977), 1 volume of 12.5 g/L bactopeptone + 5 g/L TC yeastolate (5× BPYE), and 10% fetal bovine serum. The stock M3 medium was a 1.25× concentrate of the published formula. Transfections for either transient expression or stable line selection were performed using Lipofectin reagent (Life Technologies, Gaitherburg, MD) as follows: subconfluent S2 cells (1–2 × 10^6/ml) were collected and washed twice with stock M3 to remove serum. A small aliquot of cells (10^7 per dish below) was immediately added to a mixture of Lipofectin (30 μl/ml) and DNA (20 μg/ml) in stock M3 (1 ml each per 10^7 cells) in 15 ml polystyrene centrifuge tubes. The cells were incubated for 2–3 h at room temperature (20–25°C) with gentle mixing every 30 min, pelleted, washed twice with stock M3, resuspended in 10 ml complete medium per dish, and transferred to 100-mm bacteriological grade petri dishes. Cells were collected for expression assays or transfer to selective medium 24–60 h post-transfection. To generate stable lines, pP_{ac}Hph and the AChE expression plasmid were co-transfected at a ratio of 5:1, the opposite of the ratio used in most protocols for mammalian cells (Ashburner, 1989), and 10^7 cells were suspended in 30 ml of selective medium (complete medium supplemented with 0.2 mg/ml hygromycin B; Calbiochem, La Jolla, CA) and divided into 6-well plates. Large groups of colonies were formed after 10–14 days, and pooled cells from single wells were cloned or subcultured for several passages in the presence of selective medium before cloning. Clones were isolated in 0.5% low melting temperature agarose (SeaPlaque GTG-FMC) in a complete medium lacking the BPYE with an irradiated feeder layer of S2 cells (10^6/ml) stably transfected with pP_{ac}Hph alone. Colonies (2 mm) were picked and grown in 24-well plates with feeder cells at 10^6/ml in complete selective medium, then transferred to 6-well plates without feeder cells. Clones were assayed for AChE when they reached confluency, and lines with high activity were kept for large-scale culturing at 0.2–5 × 10^6 cells/ml.

AChE Assay

The catalytic activity was determined by the spectrophotometric method of Ellman *et al.* (1961) as modified by Rosenberry and Scoggin (1984) utilizing 0.5 mM acetylthiocholine iodide or, where noted, 0.5 mM butyrylthiocholine iodide as a substrate. One unit of AChE is defined as the amount catalyzing the hydrolysis of 1 μmol acetylthiocholine per minute at 20°C.

AChE Extraction and Nondenaturing Polyacrylamide Gel Electrophoresis (ND-PAGE)

To detect AChE in crude membrane extracts, S2 cells (typically 1–3 million) were washed free of cell culture medium three times with phosphate-buffered saline (PBS; 137 mM NaCl, 2.7 mM KCl, 10 mM dibasic sodium phosphate, 1.8 mM monobasic potassium phosphate, pH 7.0) then lysed in 5 pellet-volumes of pH 6.9 DSS buffer (20 mM sodium phosphate, 150 mM NaCl, 5 mM EDTA, 1 mM EGTA, 1% Triton X-100, 5 mM *N*-ethylmaleimide, and 1.0 μg/ml each of leupeptin and pepstatin). For comparison of solubility, cells were also extracted in a similar buffer containing 60 mM *n*-octyl β-D-glucopyranoside (octylglucoside) instead of Triton X-100. After 5 min at room temperature or on ice, lysates were microfuged at 13,000 × *g* for 5–10 min and supernatants were taken for AChE assay and further analysis. To cleave the GPI anchor, aliquots were mixed with 15 μg/ml purified *Bacillus thuringiensis* phosphatidylinositol-specific phospholipase C (PIPLC) (Deeg *et al.*, 1992) for 15–30 min at room temperature. Extracts subjected to disulfide reduction were diluted into DSS buffer at pH 8.6 containing 10 mM dithiothreitol (DTT). Aliquots containing ~3 mU AChE were adjusted to 6 μl with DSS buffer to which glycerol had been added to 10% and subjected to ND-PAGE in 0.5% Triton X-100 as described (Toutant *et al.*, 1990) with the following modifications: a vertical 1.5-mm slab mini-gel was used rather than a horizontal unit, and gels were run for 150 V × h. Histochemical detection of AChE was performed according to the method of Karnovsky and Roots (1964) except that 0.1 M maleate (pH 6.0) replaced the 0.1 M acetate buffer to reduce background staining (Tago *et al.*, 1986).

Triton X-114 Partitioning

A 12% Triton X-114 stock was prepared as described (Bordier, 1988). Washed cells were lysed on ice in DSS-2 buffer (DSS buffer with 2% Triton X-114 in place of Triton X-100) and lysates were microfuged at 13,000 × *g* at 4°C for 5 min. Supernatant aliquots were treated with or without 10–15 μg/ml PIPLC and partitioned by warming to 37°C for several minutes and microfuging for 30 s. The aqueous phase was removed and replaced with fresh ice-cold detergent-free buffer to dissolve the detergent phase, and the mixture was repartitioned. The pooled aqueous phases and the detergent phase were assayed for AChE activity. GPI-anchored/secreted AChE heterodimers were quantitated as follows: 8 × 10^7 SEC1/3 cells were extracted with 5 pellet-volumes of DSS-2 buffer that was prepared at pH 8 and contained 5 mM *N*-ethylmaleimide. The cleared lysate was partitioned at 37°C and the detergent phase was washed twice with ice-cold pH 8 buffer lacking Triton and *N*-ethylmaleimide. The final detergent phase was then subjected to reduction by replacing the aqueous phase with 5 mM DTT in pH 8 buffer. After 20 min at room temperature, free sulfhydryls were quenched by adding *N*-ethylmaleimide to 10 mM. The reduced sample was then partitioned at 37°C. The aqueous and detergent phases were then assayed for AChE activity at a dilution of 1:100, where there was no interference from reaction of DTT or *N*-ethylmaleimide with the AChE substrate or reaction products, respectively.

Purification of AChE Expressed in Cell Culture and Preparation of Affinity-purified Antisera

SEC1 from the culture medium of clone S2-SEC1/3 and wild-type GPI-AChE from Sf9 cells infected with a recombinant baculovirus expressing the pE18 cDNA insert (Thomas, Eastman, Incardona, and Rosenberry, unpublished data) were purified by affinity chromatography on acridinium resin (Rosenberry and Scoggin, 1984). Rabbit antisera to *Drosophila* AChE (anti-dAChE) were produced by Pocono Rabbit Farm and Laboratories, Canadensis, PA. The purified GPI-AChE (4 mg) was used for initial subcutaneous immunizations of two rabbits and the first boost, and all subsequent boosts employed purified SEC1. The antiserum (10 ml) was partially purified by chromatography on CM AffiGel Blue (Bio-Rad, Richmond, CA) to eliminate serum proteases and albumins. For affinity purification of anti-dAChE, purified SEC1 (8 mg) was coupled to 1 ml of Affi-Gel 15 resin (Bio-Rad), and 25 ml of partially purified antiserum was applied to the AChE/AffiGel column. Bound immunoglobulins

were eluted with 0.1 M glycine (pH 2.5), 10% ethylene glycol, and fractions were neutralized with 1 M Tris (pH 8). Peak fractions of anti-dAChE were identified by A_{280} and by immunocytochemistry on cryostat sections of adult heads.

SDS-PAGE, Western Blotting, and Immunodetection

AChE samples were subjected to SDS-PAGE (Laemmli, 1970) with or without disulfide reduction (10 mM DTT) on 1.5-mm slab gels containing 7.5% acrylamide at 40 mA for 2 h. Protein bands were transferred by electroblotting to BA-83 nitrocellulose (Schleicher and Schuell, Keene, NH) and stained briefly with Ponceau S (Serva; 0.2% in 3% tricholoroacetic acid) before immunolabeling. The blot was incubated with anti-dAChE diluted 1:5000 in PBS plus 0.05% Tween-20 (TPBS) containing 5% nonfat dry milk for 2–4 h at room temperature and then transferred to peroxidase-conjugated goat anti-rabbit secondary antibody (Jackson ImmunoResearch, West Grove, PA) (1:2500 in TPBS) for 1–2 h incubation at room temperature. Peroxidase activity was developed in a substrate solution consisting of 16.7% methanol, 0.5 mg/ml 4-chloronaphthol (Polysciences, Warrington, PA), and 0.0125% H_2O_2 in PBS.

Immunocytochemistry on S2 Cells

Aliquots of cells (~3×10^6) were washed twice and resuspended in pH 7.0 PBS (1 ml). Cells examined without PIPLC treatment were attached to microscope slides coated with poly-L-lysine before fixation. Cells incubated with PIPLC (4 μg/ml) for 30 min at 25°C and washed three times with PBS would not adhere to poly-L-lysine, so fixation was carried out in suspension. Samples were fixed for 20 min in 0.1 M phosphate buffer (pH 7) containing fresh 4% paraformaldehyde, washed once in PBS, treated with 20 mM glycine in PBS for 15 min to quench excess aldehydes, and washed three times in PBS. Some samples were then permeabilized with 0.4 mg/ml saponin (Calbiochem) plus 0.4% bovine serum albumin (Sigma, St. Louis, MO) for 10 min. Samples were incubated for 1 h at room temperature with primary anti-dAChE diluted 1:2500 in PBS containing 0.1% bovine serum albumin and, for permeabilized cells, 0.4 mg/ml saponin, washed three times with PBS, and further incubated for 1 h at room temperature in rhodamine-conjugated goat anti-rabbit secondary antibody (Jackson ImmunoResearch) diluted 1:100 in the same buffer employed for the primary antiserum except that 1% normal goat serum was added. All samples were then washed three times in PBS and mounted under a coverslip in 50% glycerol in PBS plus 1% *n*-propyl gallate. Immunostained cells were viewed and photographed on a Nikon Microphot FX.

Sucrose Gradient Centrifugation

Isokinetic sucrose gradients (5–20% w/w) were prepared in 10 mM sodium phosphate (pH 7.0), 1 M NaCl, and 1% Triton X-100 and centrifuged in a Beckman SW-41Ti rotor (Younkin *et al.*, 1982). Aliquots of DSS extracts of S2 cell lines (10 U of AChE) adjusted to 50 μl with DSS buffer were mixed with 70 μl of catalase (4 mg/ml in DSS buffer) and loaded on 11-ml gradients. Fractions (0.34 ml) were collected and assayed for AChE activity; catalase was measured by absorbance at 406 nm. Sedimentation coefficients were calculated relative to that of catalase (11.4 S).

RESULTS

Construction of Secreted and Transmembrane-anchored AChEs

The strategy used to generate the two mutant forms of *Drosophila* AChE employed synthetic linkers and small restriction fragments encoding stable transmembrane peptides. Although the mature C-terminus of *Drosophila* AChE has not been determined, homology with the GPI-anchored form of *Torpedo* AChE suggests that it is at or just downstream of C^{615}. Since this cysteine is involved in the interchain disulfide bond of the *Drosophila* AChE dimer (Mutero and Fournier, 1992), it was retained in all constructs. Based upon previous constructs of DAF and PLAP (Berger *et al.*, 1988; Caras *et al.*, 1989), one would predict that truncation of most of the C-terminal peptide that serves as a GPI-anchoring signal would result in a secreted AChE. One truncation was produced by cleavage at the *Xmn*I site in pE18 between codons 621 and 622 and insertion of a commercial *Nhe*I linker sequence to generate pSEC1 (Figure 1A). The third stop codon in the linker is in frame with codon 621, and three new codons are added that result in a new C-terminal sequence C^{615}DGDSGSLAS that lacks the final 25 residues of the original signal peptide. Despite the large truncation, a small but significant amount of the expressed SEC1 enzyme remained GPI-anchored (see below). Therefore, a second truncated AChE (SEC2) was designed in which an additional four residues were deleted. Construction of pSEC2 (Figure 1B) utilized a *Tfi*I site within codon 618, and the stop codon and the C-terminal Ser residue were provided by the same *Nhe*I linker used for pSEC1. The resulting C-terminal sequence was C^{615}DGDSS (Figure 1C).

Insertion of the *Nhe*I linker into pE18 not only resulted in the truncation in SEC1 but provided a unique site for insertion of restriction fragments encoding transmembrane peptides that immediately precede the linker stop codons. Several criteria were considered in selecting an appropriate transmembrane sequence (see DISCUSSION). Initial studies with the transmembrane domain of the VSV G failed to produce a chimeric protein with AChE activity, but an active chimeric AChE was obtained with the transmembrane domain of HSV-1 gC. A restriction fragment encoding the 22-residue transmembrane and 11-residue cytoplasmic domains of HSV-1 gC (Frink *et al.*, 1983) was inserted into the *Nhe*I site of pSEC1 to create a construct in which the transmembrane sequence is fused to Ser^{624} (Figure 1C).

The Secreted and Membrane-bound AChE cDNAs Produce Functional Enzymes with Indistinguishable Catalytic Properties when Expressed in Cultured Cells

To characterize the cellular processing and enzymatic function of the altered AChEs, cDNAs corresponding to the four constructs (Figure 1C) were expressed in *Drosophila* S2 cells. The S2 cell line possesses no endogenous AChE activity nor immunoreactivity (our unpublished results). Constitutive expression was achieved with the *Drosophila* expression vector pP_{ac}, under control of the *Actin 5C* promoter (Krasnow *et al.*,

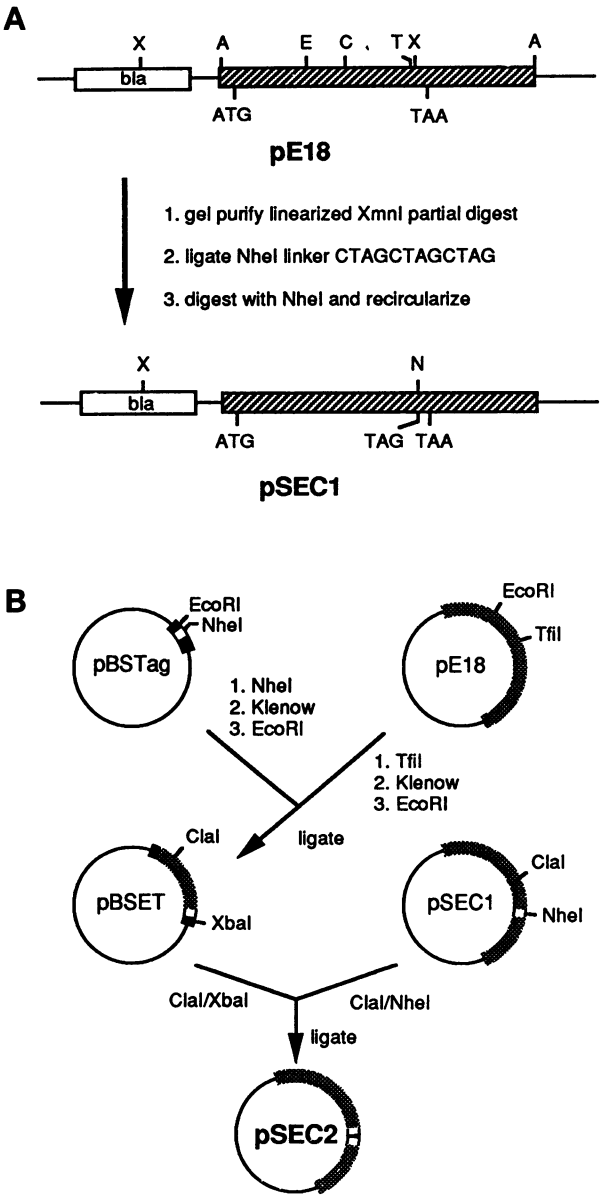

C

```
GPI:  CDGDSGSASIPRLQLLGIAALIYICAALRTKRVF

SEC1: CDGDSGSLAS

SEC2: CDGDSS

TM:   CDGDSGSLASEWVGIGVLAAGVLVVTAIVYVVRTSQSRQRHRR
```

Figure 1. Construction strategies for the mutant AChEs and their C-terminal sequences. (A) Construction of pSEC1. The C-terminal signal peptide was truncated by insertion of an *Nhe*I linker containing stop codons in three frames into the *Xmn*I site in the 3′ end of the *Ace* cDNA (hatched box) contained in pE18. Although there is also an *Xmn*I site in β-lactamase (bla, unfilled box), insertions there are not recovered following selection on ampicillin. 1989). Several lines for each construct with high enzymatic activity were isolated and maintained in selective medium (Table 1). Lines E18/3 and GC/3, which expressed GPI-AChE and TM-AChE proteins at typical levels, respectively, both contained about 0.4 U (300 ng) of AChE per million cells. Line SEC1/3, which expressed secreted AChE corresponding to SEC1 (Figure 1C), had about 0.2 U of cell-associated AChE in Triton X-100 lysates, but AChE levels in the culture medium accumulated to as high as 140 U/ml (100 μg/ml) after 6 days of continuous growth. The SEC2-secreting line SEC2/4 expressed a lower level of cell-associated AChE (0.03 U per million cells) than SEC1/3 and typically gave levels of 20 U/ml in the culture medium. Although the E18/3 and GC/11 lines expressing membrane-bound AChEs also released detectable amounts of AChE activity to the culture medium, the levels achieved were 2–3 orders of magnitude lower than those for SEC1 and SEC2 lines. Forty milligrams of SEC1 was purified by affinity chromatography from 800 ml of medium from S2-SEC1/3 cells to produce antisera for experiments described below.

Because GPI-anchored proteins in many mammalian cells form complexes that are insoluble in cold Triton X-100 (Brown and Rose, 1992; Sargiacomo *et al.*, 1993), we compared the extraction of GPI- and TM-AChE in cold buffer containing Triton X-100. We found that both proteins were essentially completely soluble in Triton X-100 at either 4°C or room temperature (our unpublished observations), even when using careful lysis with a protocol used for isolating the complexes from MDCK cells (M. Lisanti, personal communication). Furthermore, the solubility of both proteins in octylglucoside was identical to their solubility in Triton X-100 (our unpublished results). GPI-anchored proteins from mammalian cells insoluble in

(Figure 1 cont.) Restriction sites are *X*, *Xmn*I; *N*, *Nhe*I; *A*, *Asp*718; *E*, *Eco*RI; *C*, *Cla*I; and *T*, *Tfi*I. (B) Construction of pSEC2. The same *Nhe*I linker utilized in pSEC1 was first inserted into the *Sma*I site of pBluescript KS(+) (Stratagene) to generate pBSTag. pE18 was cut with *Tfi*I after the first base of codon 618, the 5′ overhang was filled with the Klenow fragment of DNA polymerase I, and a 1.1-kb *Eco*RI/Tfi I fragment was ligated into pBSTag that had been linearized with *Nhe*I, filled with Klenow, and cut with *Eco*RI. In the resulting pBSET, the blunt end ligation of the *Tfi* and *Nhe* sites regenerated Ser^{619} and provided an additional Ser codon immediately preceding the second stop codon of the linker. This segment of coding sequence was returned to the full-length cDNA by ligation of a 630-bp *Cla*I/*Xba*I fragment from pBSET to the *Cla*I and *Nhe*I compatible sticky ends of pSEC1, generating pSEC2. pSEC2 thus has a duplication of the *Nhe*I linker. *Ace* cDNA is represented by stippling, linker sequences by unfilled boxes, and pBluescript polylinker sequences by solid black. (C) C-terminal sequences of wild-type (GPI) AChE, the secreted forms (*SEC1* and *SEC2*), and transmembrane (TM) AChE, starting from Cys^{615}. DNAs are not drawn to scale.

Table 1. AChE activity expressed by cloned stably-transfected S2 lines

AChE form	Line	Units AChE/10^6 cells	Units AChE/ml culture medium
GPI-AChE	E18/3	0.4	0.6
TM-AChE	GC/11	0.03	0.07
TM-AChE	GC/8	0.1	ND[a]
TM-AChE	GC/3	0.4	ND
TM-AChE	GC/12	2.0	ND
SEC1	SEC1/3	0.2	100[b]
SEC2	SEC2/4	0.03	20

Hygromycin-resistant stable transfectants expressing each of the four AChE constructs were cloned as described under METHODS AND MATERIALS. To determine AChE expression levels, Trypan blue-excluding cells were counted (>90%), pelleted, and extracted with DSS buffer. Crude extracts and aliquots of culture medium were assayed for AChE as described under MATERIALS AND METHODS. AChE in the culture medium was assayed 6 days after placing the cells into AChE-free medium. Values presented are from single determinations.

[a] ND, not determined.

[b] Line SEC1/3 typically produced AChE levels of 80–100 units/ml over this period, but levels as high as 140 units/ml were achieved.

cold Triton X-100 are essentially completely soluble in octylglucoside (Brown and Rose, 1992).

To assess whether these structural alterations affected the catalytic activity, we compared substrate hydrolysis rates for both acetylthiocholine and butyrylthiocholine. At saturating substrate concentrations, AChE from *Drosophila* hydrolyzes butyrylthiocholine at about 50% of the rate for acetylthiocholine, a substrate specificity intermediate to that for vertebrate acetycholinesterases and butyrylcholinesterases (Gnagey *et al.*, 1987). Observed ratios of butyrylthiocholine to acetylthiocholine hydrolysis rates for AChEs expressed in S2 cells were as follows: 0.58 ± 0.03 for GPI-AChE; 0.57 ± 0.09 for TM-AChE; and 0.56 ± 0.03 for SEC1 (means of at least three determinations). These values are essentially identical to the ratio of 0.56 ± 0.02 observed for the native GPI-AChE purified from adult fly heads (Gnagey *et al.*, 1987). These data are consistent with previous observations on AChEs from other species that indicated that alterations in the mode of membrane anchoring have no effect on AChE catalytic function (Vigny *et al.*, 1978).

ND-PAGE Analysis of TM-AChE Shows that It Is Amphiphilic and PIPLC Resistant

To assess the quaternary structure and detergent-binding properties of the AChE constructs, crude Triton X-100 extracts of the S2 lines were subjected to ND-PAGE and AChE was detected by a histochemical activity stain. A primary determinant of the mobility of an amphiphilic protein in this gel system is the binding of Triton X-100 micelles, and conversion of an amphiphilic, detergent-binding protein to a hydrophilic form that does not bind detergent is easily demonstrated (Toutant *et al.*, 1990). Figure 2 illustrates these points with GPI-AChE produced by line E18/3: the slowest migrating form of AChE was the amphiphilic dimer G_2a (Figure 2, lane 1), with the amphiphilic monomer G_1a produced by disulfide reduction running slightly faster (Figure 2, lane 2). Cleavage of the GPI anchor with PIPLC produced hydrophilic dimer G_2h that migrated significantly faster (Figure 2, lane 3); upon reduction (Figure 2, lane 4) the hydrophilic monomer G_1h ran faster yet. Figure 2 (lanes 5–8) shows that, as predicted, TM-AChE produced by line GC/3 appeared to correspond to an amphiphilic disulfide-linked dimer that was resistant to PIPLC. Upon reduction its mobility increased slightly and aligned with G_1a (Figure 2, compare lanes 5 and 6), suggesting that a dimeric structure was retained by the chimera and that the intersubunit disulfide bond was accessible to reducing agent. No hydrophilic enzyme was produced by PIPLC treatment (Figure 2, lanes 7 and 8). The faint amount of hydrophilic enzyme at the position of G_2h with the TM-AChE construct probably was due to proteolysis, as its amount did not increase with PIPLC treatment (Figure 2, compare lanes 5 and 7). Interestingly, TM-AChE seemed to be more resistant to reduction: GPI-AChE was readily reduced by

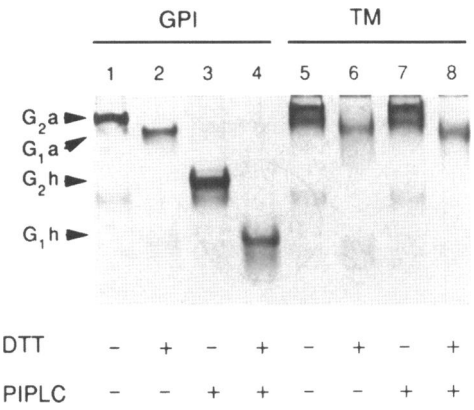

Figure 2. ND-PAGE analysis of GPI-AChE and TM-AChE. Crude DSS lysates were prepared from the S2 lines expressing each AChE and subjected to the indicated treatments as described under MATERIALS AND METHODS. Samples (3 mU) were electrophoresed in gels containing 0.5% Triton X-100 and visualized by a histochemical activity stain that produces a brown precipitate. (GPI) GPI-AChE expressed by line E18/3. Lane 1, untreated extract; lane 2, reduced with 10 mM dithiothreitol; lane 3, treated with PIPLC; and lane 4, reduced with 10 mM DTT and treated with PIPLC. (TM) TM-AChE expressed by GC/3 cells. Lane 1, untreated extract; lane 2, reduced with 10 mM DTT at pH 8.6; lane 3 treated with PIPLC; and lane 4, reduced and treated with PIPLC. G_2a, amphiphilic dimer; G_1a, amphiphilic monomer; G_2h, hydrophilic dimer; and G_1h, hydrophilic monomer.

10 mM DTT at pH 7, but TM-AChE could only be reduced efficiently at a pH > 8 (our unpublished observations). This ND-PAGE analysis provides strong evidence that TM-AChE is a chimeric transmembrane form: it was amphiphilic and, as shown by its resistance to PIPLC, none of it appeared to receive a GPI anchor.

To show the quantitative resistance of TM-AChE to PIPLC, we assayed the AChE activity released by PIPLC treatment of intact cells expressing GPI- or TM-AChE. Cells from lines E18/3 and GC/3 were treated with PIPLC or with buffer alone and washed, and the remaining cell-associated AChE activity was determined. As shown in Table 2, 72% of GPI-AChE was cleaved from the surface of intact cells. The apparent resistance of nearly 30% of this enzyme probably reflects its residence in an intracellular compartment (see below). TM-AChE, however, showed no release from intact cells with PIPLC. A second method used to quantitate GPI cleavage by PIPLC was Triton X-114 phase partitioning. Upon warming a Triton X-114 solution above its cloud point, it separates into a detergent phase enriched in amphiphilic or hydrophobic proteins and a detergent-poor aqueous phase. PIPLC sensitivity was measured by a shift of AChE activity from the detergent phase to the aqueous phase. As shown in Table 3, 75% of the GPI-AChE extracted from E18/3 cells was found in the detergent phase. Although the 25% that remained in the aqueous phase was significant, this enzyme was shown to have the GPI anchor by its mobility and susceptibility to PIPLC on ND-PAGE (our unpublished results; similar observations have been made for native AChE in fly head extracts). Only 1.3% of the GPI-AChE activity was found in the detergent phase after PIPLC treatment, indicating that GPI-AChE is essentially 99% susceptible to PIPLC when the cells are solubilized in detergent. The behavior of TM-AChE in Triton X-114 proved to be surprising: it partitioned nearly equally between the aqueous and detergent phases. Such an observation was also made for a chimeric placental alkaline phosphatase anchored by the transmembrane domain of VSV G (Berger *et al.*, 1989). Treatment with PIPLC, however, had no effect on the partition distribution of TM-AChE, consistent with the indication from the ND-PAGE analysis and treatment of intact cells that PIPLC has no effect on TM-AChE.

Table 2. AChE activity associated with intact cells before and after PIPLC treatment

AChE form	Units AChE (−)PIPLC	Units AChE (+)PIPLC	% cleaved
GPI-AChE	0.28 ± 0.02	0.078 ± 0.002	72 ± 2
TM-AChE	0.37 ± 0.06	0.39 ± 0.01	0

Cells expressing GPI-AChE (E18/3) and TM-AChE (GC/3) were treated with (+) or without (−) PIPLC as described under MATERIALS AND METHODS. DSS extracts were prepared from 3–6 × 10^6 cells after washing away PIPLC and any cleaved AChE, and aliquots representing 1/10 of the extract volume were assayed for AChE activity. Units AChE are as defined under MATERIALS AND METHODS. Values are the means and standard errors from triplicate measurements.

Table 3. Percentage of AChE activity present in the hydrophobic phase of Triton X-114 before and after PIPLC treatment

AChE form	PIPLC	% Hydrophobic	% Cleaved
GPI-AChE	−	75.4 ± 3.4	NA[a]
GPI-AChE	+	1.3 ± 0.1	98.7
TM-AChE	−	49.5 ± 2.2	NA
TM-AChE	+	51.1 ± 4.7	0

Lysates were prepared from the same cell lines represented in Table 2 using DSS-2 buffer containing Triton X-114 instead of Triton X-100 as described under MATERIALS AND METHODS. Aliquots of the lysates were treated with (+) and without (−) PIPLC. After partitioning the extracts at 37°C, the total aqueous and detergent phases were assayed for AChE activity. Values are the means and standard errors of percentages relative to the sum of activities in aqueous and detergent phases obtained from triplicate measurements.

[a] NA, not applicable.

Sucrose Gradient Sedimentation of TM-AChE Shows that It Is a Disulfide-linked Dimer

Although ND-PAGE results in Figure 2 suggested that TM-AChE is expressed as a dimer, sedimentation analysis provides a more rigorous estimate of size. GPI-AChE from E18/3 and TM-AChE from GC/3 were extracted in DSS buffer and sedimented in 5–20% sucrose gradients in the presence of 1% Triton X-100. A peak at 6.7 S observed for GPI-AChE was consistent with that found by Gnagey *et al.* (1987) for the dimeric enzyme purified from fly heads; upon reduction, the peak was shifted to 4.9 ± 0.1 S, a position consistent with monomers (Rosenberry and Scoggin, 1984). TM-AChE sedimented at 7.3 ± 0.3 S and upon reduction was shifted to 5.5 S, values indicative of dimeric AChE. Membrane-bound tetrameric AChEs typically sediment at 10–11 S, and the S value is not altered by disulfide reduction (Vigny *et al.*, 1979). The slightly greater sedimentation coefficient of TM-AChE may be explained by a decreased ability to bind detergent. Dimeric fly AChE is shifted to about 7.5 S in the absence of detergent (Gnagey *et al.*, 1987) and secreted SEC1, which should not interact with detergent, sedimented at 7.7 S. A decreased interaction with detergent by TM-AChE may also explain the fuzziness of its dimer bands on ND-PAGE (Figure 2) and its phase partitioning behavior in Table 3. Although TM-AChE may differ slightly from GPI-AChE in its interactions

with detergent, the HSV-1 gC transmembrane domain appears to mediate the association of TM AChE with membranes and does not disturb the quaternary structure of the native dimeric enzyme.

The Signal for GPI Addition Is Completely Truncated in SEC2 but Only Partially Truncated in SEC1

Figure 3A shows ND-PAGE analysis of the AChE expressed by the SEC1/3 line. As expected, the large amount of enzyme secreted to the culture medium (Table 1) corresponded to the hydrophilic dimer G_2h (Figure 3A, lane 1). However, analysis of a Triton X-100 extract of cell-associated enzyme from either transiently transfected S2 cells (our unpublished results) or line SEC1/3 provided an unexpected result. As seen in Figure 3A, lane 2, a significant band appeared at the position of amphiphilic dimer (G_2a), and a doublet of hydrophilic dimers (G_2h and G_2h') was observed. To determine if the band at G_2a was in fact GPI-anchored dimer, SEC1/3 cells were extracted in Triton X-114 and subjected to phase partitioning. The resulting aqueous phase contained predominantly the two forms of hydrophilic dimer along with a small amount of the amphiphilic dimer (Figure 3A, lane 3). Only the G_2a band partitioned into the detergent phase (Figure 3A, lane 4) and, after treatment with PIPLC, it was converted to hydrophilic dimer (Figure 3A, lane 5), a partitioning pattern identical to that observed for a Triton X-100 extract of GPI-AChE (Figure 3A, lanes 6 and 7). To rule out any possibility that the amphiphilic, PIPLC-sensitive AChE expressed by SEC1/3 cells represented a heterodimer of hydrophilic AChE with an unrelated GPI-anchored protein, we tested the sensitivity of the G_2a AChE to reduction (Figure 3B). The G_2a band present in the detergent phase of a Triton X-114 extract (Figure 3B, lane 1) was sensitive to reduction with 5 mM DTT, producing a band of amphiphilic monomer (G_1a) and a band of hydrophilic monomer (G_1h) (Figure 3B, lane 3). Furthermore, the G_1a band was converted to hydrophilic G_1h with PIPLC treatment (Figure 3B, lane 4). This indicates that the amphiphilic AChE in SEC1/3 cells is in fact heterodimeric, but the heterodimers consist of monomeric secreted AChE attached by disulfide linkage to a GPI-anchored AChE monomer, and are not bound to an unrelated GPI-anchored protein. To quantitate the percentage of heterodimeric AChE, the detergent phase of the Triton X-114 extract was reduced with DTT and repartitioned, and the resulting amphiphilic and aqueous phases were assayed for AChE activity. Twenty-five percent of the total activity of the original detergent phase was released into the subsequent aqueous phase upon reduction. This finding demonstrates that 50% of the amphiphilic AChE molecules in SEC1/3 cells are heterodimers of secreted and GPI-anchored AChE, while the other 50% is homodimeric GPI-anchored AChE.

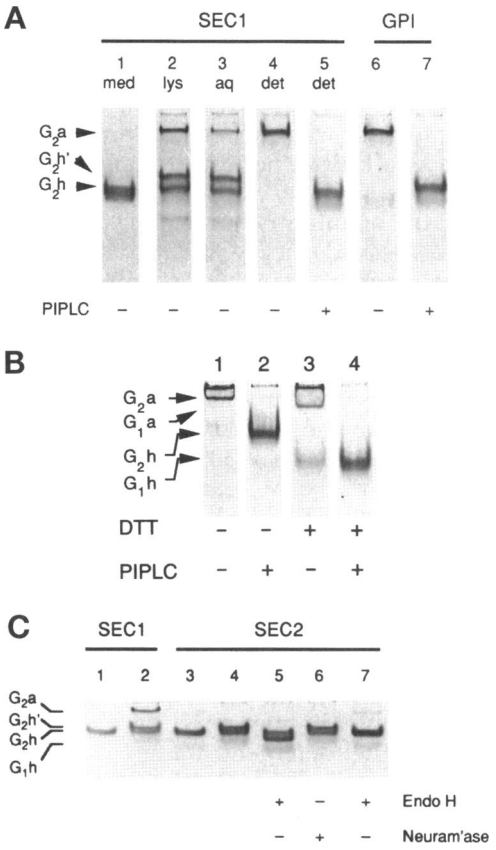

Figure 3. ND-PAGE analysis of secreted AChEs. Crude Triton X-100 extracts or culture medium of S2 cells expressing the SEC1 and SEC2 constructs were prepared and subjected to ND-PAGE as described in the MATERIALS AND METHODS and in the legend to Figure 2. (A) Lanes 1–5: SEC1 produced by SEC1/3 cells. Lane 1, culture medium; lane 2, untreated Triton X-100 extract; lane 3, aqueous phase from a Triton X-114 extract; lane 4, detergent phase of a Triton X-114 extract; lane 5, detergent phase of Triton X-114 extract treated with PIPLC; lane 6, untreated GPI-AChE from E18/3 cells; and lane 7, GPI-AChE treated with PIPLC. (B) Lanes 1–4, detergent phase of partitioned Triton X-114 extract of SEC1/3 cells. Lane 1, untreated detergent phase; lane 2, detergent phase treated with 8 μg/ml PIPLC; lane 3, detergent phase reduced with 5 mM DTT; and lane 4, detergent phase treated with 5 mM DTT and 8 μg/ml PIPLC. (C) Lanes 1–2: SEC1; lanes 3–8: SEC2 expressed by SEC2/4 cells. Lane 1, culture medium; lane 2, Triton X-100 extract; lane 3, culture medium; lane 4, Triton X-100 extract; lane 5, Triton X-100 extract treated with 5 mU endo H for 3 h at room temperature; lane 6, a parallel aliquot of Triton X-100 extract treated with 5 mU neuraminidase for 3 h at room temperature; and lane 7, SEC2 in culture medium treated with 5 mU endo H. Band labels are described in the legend to Figure 2; the slower migrating hydrophilic dimer band is designated G_2h'. The faint band close to G_2a in lanes loaded with culture medium was due to tetrameric bovine serum cholinesterase from the medium supplement (our unpublished results).

The ND-PAGE profile of SEC2, which is four residues shorter than SEC1, is compared with that of SEC1

in Figure 3C. Secreted SEC2 AChE (Figure 3C, lane 3) appeared identical to secreted SEC1 (Figure 3C, lane 1). A Triton X-100 extract of cells expressing SEC2 showed no amphiphilic enzyme (Figure 3C, lane 4), in contrast to an extract of SEC1-expressing cells (Figure 3C, lane 2). Moreover, Triton X-114 partitioning of SEC2 extracted from S2 cells showed absolutely no activity in the hydrophobic phase (our unpublished results). The further truncation of four residues appeared to eliminate completely any GPI addition signal. Interestingly, cell-associated SEC2 also exhibited the two hydrophilic AChE bands (G_2h and G_2h′) that were found associated with cells expressing SEC1. Three observations suggested that the G_2h′ band may be an incompletely processed precursor in the secretory pathway. 1) The faster moving G_2h band comigrated with the presumably fully processed enzyme that was found in the culture medium. 2) Presumably fully processed GPI-AChE yields exclusively the G_2h band upon treatment with PIPLC (Figure 3A, lanes 5 and 7). 3) The G_2h′ band was sensitive to treatment with endoglycosidase H (endo H; Figure 3C, lane 5), which produced a new band that migrated faster than the band from the medium in Figure 3B, lane 3. Note also that the G_1h band was endo H-sensitive, consistent with previous assignments of G_1 AChEs as immature precursors (Rotundo, 1988; Toutant *et al.*, 1990). Neither G_2h nor G_2h′ was sensitive to neuraminidase (Figure 3C, lane 6), consistent with reports that insect cells do not add sialic acid to N-linked glycans (Butters *et al.*, 1981; Hsieh and Robbins, 1984). Although it is possible that the mobilities of both cellular G_2h and G_2h′ were increased after treatment with endo H, this seems unlikely because the AChE found in the culture medium was endo H-resistant (Figure 3C, lane 7). Although some mature proteins expressed in insect cells have been found to contain a mixture of endo H-sensitive and resistant oligosaccharides (Hsieh and Robbins, 1984; Kuroda *et al.*, 1990), it is clear that mature, secreted SEC1 and SEC2 have predominantly trimmed N-glycans.

Previous studies on C-terminal amino acid sequence signals mediating GPI attachment have concluded that a large truncation like that in SEC1 results in no GPI addition (Berger *et al.*, 1988; Caras *et al.*, 1989). However, these studies have relied on metabolic radiolabeling of GPI anchor components combined with autoradiography, and it is possible that the exquisite sensitivity of AChE histochemical detection permits small amounts of GPI-anchored protein to be observed in our experiments. Quantitation of AChE activity associated with the aqueous and detergent phases of partitioned Triton X-114 lysates of line SEC1/3 showed that 13.5 ± 0.1% of the cell-associated SEC1 was amphiphilic. Because this value seemed surprisingly high, we wanted to determine whether it reflected a slow accumulation and low turnover rate of a small amount of GPI-anchored AChE. To assess the percentage of total AChE synthesized that received a GPI anchor, we performed Triton X-114 partitioning in combination with a pulse-chase experiment designed to assay the rates of synthesis of cell-associated and secreted SEC1. SEC1/3 cells were treated with a membrane permeable irreversible AChE inhibitor (methanesulfonyl fluoride, MSF), washed free of inhibitor, and returned to medium. AChE activity was then determined over a 23-h period in the medium and in Triton X-114 cell extracts after phase partitioning. Total AChE synthesized was calculated as the sum of the activities in the three pools shown in Figure 4. Before MSF treatment, 40 mU of AChE per million cells or 15% of the cell-associated AChE was found in the detergent phase and defined as "hydrophobic," although as shown in Figure 3B only 75% of this AChE is GPI-anchored. At 45 min after MSF treatment, 3 mU of AChE or roughly 10% of the total newly synthesized AChE was hydrophobic. This percentage was maintained at 2 h and declined only slightly to 5–6% at 3.5 h and 6.5 h. It is notable that the cellular hydrophilic AChE accumulated at a slower rate than the GPI-anchored cellular hydrophobic form. Over this 6.5-h recovery period the percentage of hydrophobic AChE in the cellular pool fell from 45% to 36%, in contrast to the 15% in untreated cells. GPI-anchoring of SEC1 therefore is relatively efficient and, after subtracting the percentage contributed by heterodimers, appears to occur on about 4–7.5% of the total AChE synthesized. This result is unexpected and unprecedented in light of current models for the C-terminal sequence rules governing GPI addition to nascent proteins.

SDS-PAGE Analysis of AChEs Produced by the S2 Lines Demonstrates Normal Post-translational Processing

Native AChE extracted from *Drosophila* is a 140-kDa dimer (Gnagey *et al.*, 1987). Unlike vertebrate AChEs, this AChE subunit is translated as a 70-kDa precursor that is then proteolytically cleaved into 16-kDa and 55-kDa fragments that remain noncovalently associated. Figure 5 shows a Western blot of native fly head AChE and the four constructs expressed in S2 cells. The predominant band after disulfide reduction of AChE from adult flies was the 55-kDa subunit (Figure 5, lane 1). GPI-AChE from S2 cells did not undergo the proteolytic cleavage as readily, and about equal amounts of 70-kDa and 55-kDa bands were observed (Figure 5, lane 2). In addition, a smaller approximately 50-kDa band was apparent that became more pronounced on storage of GPI-AChE purified from S2 cells (our unpublished observations). TM-AChE and both secreted forms showed patterns similar to GPI-AChE (Figure 5, lanes 3–5). The TM-AChE (Figure 5,

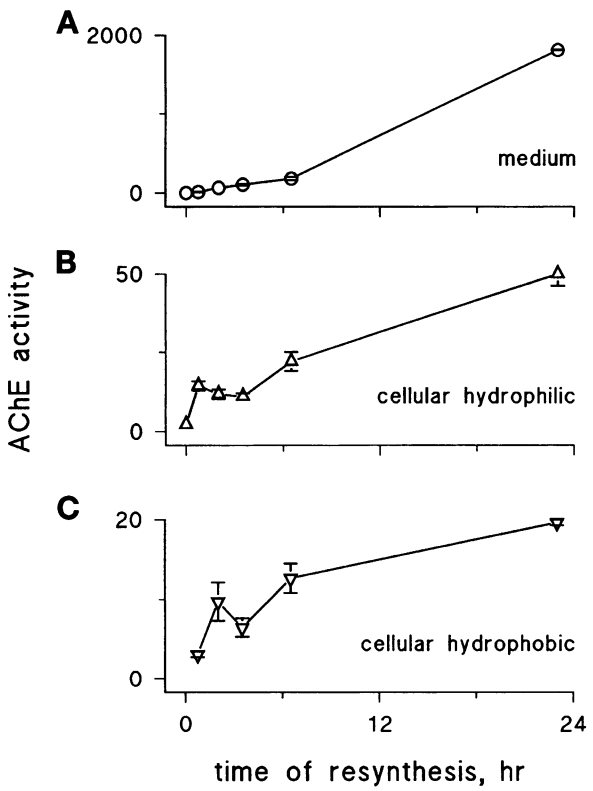

Figure 4. Quantitation of GPI-anchored AChE synthesized by SEC1/3 cells after MSF treatment. Confluent cells (10^8) from line SEC1/3 were treated for 1 h with 4 mM MSF. The cells were washed and placed in fresh medium that contained fetal bovine serum which had been treated with 4 mM MSF for 6 h and dialyzed against PBS to inhibit serum cholinesterase. Newly synthesized SEC1 was examined at several time points up to 23 h after MSF treatment. Treated cells recover and continue to grow after a slight delay in cell division, although the activities of cell-associated hydrophilic and hydrophobic AChE 23 h after MSF treatment reached only 25% and 50%, respectively, of those in the untreated control (our unpublished observations). At each point trypan blue-excluding cells (~90%) were counted and an aliquot removed, washed, and extracted in buffer containing Triton X-114. Extracts were partitioned as described in MATERIALS AND METHODS and phases assayed for AChE activity; in addition, an aliquot of the culture medium was assayed. Points represent milliunits of AChE activity normalized to 10^6 cells and show the means and standard errors of triplicate determinations. (A) SEC1 secreted into the culture medium. (B) Cell-associated SEC1 partitioning in the aqueous phase, defined here as the "hydrophilic" component. (C) Cell-associated SEC1 partitioning in the detergent phase, defined here as the "hydrophobic" component.

lane 3) appeared slightly larger than GPI-AChE, consistent with the fact that the TM segment is about 2 kDa larger that the GPI anchor. Both SEC1 and SEC2 obtained from culture medium (Figure 5, lanes 4 and 5, respectively) appeared to have a greater percentage of the uncleaved 70-kDa form and showed little of the 50-kDa fragment. Because of the inefficient cleavage of the 70-kDa precursor, three additional bands were seen in the nonreduced samples of the S2 AChEs. GPI-AChE and TM-AChE (Figure 5, lanes 6 and 7, respectively) both showed dimers of 140 kDa, 125 kDa, and 110 kDa with the latter predominant. These are, respectively, homodimers of 70-kDa subunits, heterodimers of 70- and 55-kDa subunits, and homodimers of 55-kDa subunits. Because there is a smaller percentage of 55-kDa subunit for SEC1 and SEC2, the predominant dimers observed are the 140- and 125-kDa bands (Figure 5, lanes 8 and 9, respectively). These data indicate that the four AChE constructs are processed similarly by S2 cells, with only a minor decrease in the extent of proteolytic cleavage of the secreted forms.

Immunocytochemistry of S2 Cell Lines Expressing the Four AChE Constructs

Immunofluorescence analysis of the S2 cell lines with AChE antisera provided information about the expression of AChE constructs on the cell surface. Cells from the four lines were fixed in paraformaldehyde and immunolabeled as shown in Figure 6. The pattern of cell surface staining for GPI-AChE (Figure 6A) and TM-AChE (Figure 6B) was similar at this level of resolution. The plane of focus was in the middle of the cells and showed a halo of immunofluorescence indicating surface expression. Another plane of focus on the surface of the cells showed an irregular punctate pattern for both enzymes (our unpublished data). Figure 6C shows that cells expressing SEC1 had immunoreactivity on the cell surface. Since this surface AChE is GPI-anchored (Figure 3), the pattern was very similar to that for the GPI-AChE cell line in Figure 6A. SEC2-expressing cells showed no cell-surface immunoreactivity (Figure 6D). In a parallel set of experiments, cells from the four lines were treated with PIPLC before fixation, and some samples were permeabilized before immunolabeling (Figure 7). PIPLC treatment greatly reduced the immunofluorescence from GPI-AChE on E18/3 cells (Figure 7A), whereas it had no effect on cells expressing TM-AChE (Figure 7B). As expected from the biochemical data in Figure 3A, the cell-surface immunoreactivity on SEC1-expressing cells was abolished by treatment with PIPLC (Figure 7C). PIPLC-treated cells expressing GPI-AChE showed significant intracellular immunoreactivity after permeabilization with saponin (Figure 7D), an observation consistent with the PIPLC resistance of as much as 30% of the total AChE activity expressed by intact cells (Table 2). The staining pattern was perinuclear, and large, intensely fluorescent vesicular structures were often observed. Cells expressing TM-AChE that were treated with PIPLC and permeabilized showed increased immunofluorescence (Figure 7E), but the intracellular signal was obscured by that remaining on the surface. When cells expressing SEC1 and SEC2 were permeabilized (SEC1, Figure 7F), in-

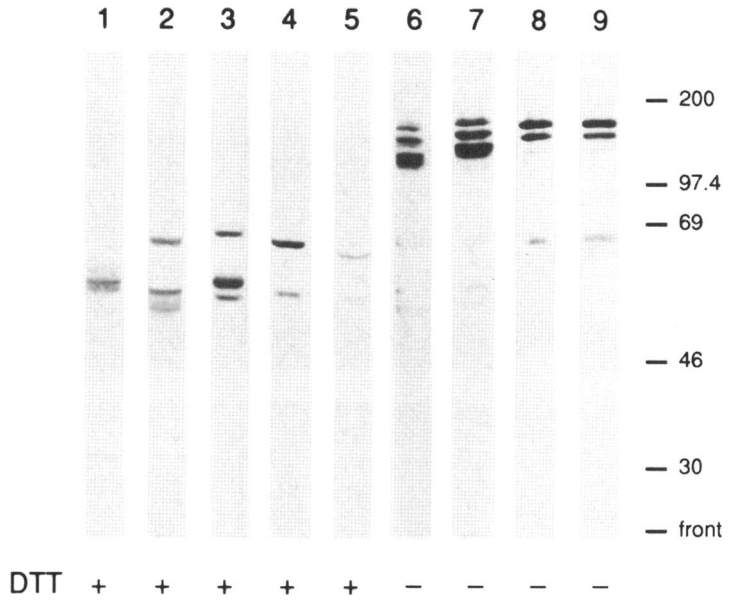

Figure 5. SDS-PAGE analysis of the AChE forms expressed in S2 cell lines. Samples corresponding to a DSS extract of 10–20 *Drosophila* heads (30 μl) or to culture medium or DSS extracts of S2 cell lines (0.14 U or 100 ng of AChE) were subjected to SDS-PAGE and Western blotting with an AChE antiserum as described in MATERIALS AND METHODS. Samples in lanes 1–5 were reduced with 10 mM DTT before electrophoresis, while those in lanes 6–9 were not reduced. Lane 1, wild-type AChE from *Drosophila* heads; lanes 2 and 6, GPI-AChE from E18/3 cells; lanes 3 and 7, TM-AChE from GC/12 cells; lanes 4 and 8, SEC1 from the culture medium of SEC1/3 cells; and lanes 5 and 9, SEC2 from culture medium of SEC2/4 cells. Migration of molecular weight standards is indicated at the right. The SEC2 70-kDa band in lane 5 was distorted because antibody binding was blocked by the presence of a large band of albumin from the culture medium revealed by Ponceau S staining before incubation with antiserum (our unpublished observations).

tracellular structures similar to those seen for GPI-AChE were intensely labeled (SEC2 not shown).

Inactivation of External AChE with Echothiophate Shows that Equivalent Levels of TM-AChE and GPI-AChE Are on the Cell Surface

Although the immunofluorescence data indicate that both GPI-AChE and TM-AChE were expressed on the cell surface, the technique does not allow quantitative comparison of the two antigens. To determine whether TM-AChE was delivered to the cell surface to the same extent as GPI-AChE, we assessed the intracellular and cell-surface pools with echothiophate (ETP). This reagent inactivates AChE essentially irreversibly by diethylphosphorylation of the active site serine, but it does not cross cell membranes at 0°C because it is cationic. ETP has been used to determine the cellular localization of AChE forms in cultured rat myotubes and rat skeletal muscle by virtue of its selective inactivation of external enzyme (Brockman *et al.*, 1982; Younkin *et al.*, 1982). We first treated solubilized GPI- and TM-AChE with various concentrations of ETP at 0°C and 25°C to determine an optimal inhibiting concentration; 10 uM was found to inhibit both enzymes at 0°C with a half-time of about 7 min. S2 cells expressing GPI-AChE (S2-E18/3) were next treated with 10 uM ETP at 0°C, and these cells together with untreated control cells were then incubated with or without PIPLC to compare the inactivated pool with that cleaved by PIPLC. As shown in Table 4, 24% of the total AChE activity remained after ETP treatment, indicating that 76% was inactivated on the cell surface. These percentages were in good agreement with the distribution of AChE activity after PIPLC treatment of the control cells: 66% was released and 24% was cell-associated. The slight loss of total activity with PIPLC treatment (10%) was due in part to incomplete recovery of cleaved AChE from the cells before washing. When the cells were treated sequentially with ETP and PIPLC, the cell-associated AChE activity (23%) was essentially identical to that for cells treated with ETP or PIPLC alone. Furthermore, only 7% of the total activity was released after the sequential treatment. Therefore, ETP did not have access to intracellular AChE while it inactivated 90% of the cell-surface AChE sensitive to PIPLC. Cells expressing TM-AChE (GC/3, GC/8, or GC/11) were processed in parallel and found to have a 73% inactivation of AChE after ETP treatment (our unpublished results), in good agreement with the inactivation of cellular GPI-AChE. In other experiments the percentages of GPI-AChE inhibited by ETP or released by PIPLC ranged in parallel from 50–75%, depending on the density and age of the cultures (our unpublished results). However, in all cases the percentages of AChE inactivated by ETP was nearly identical for GPI- and TM-AChE when the culture conditions were matched. Since lower density cultures are more likely to have increased levels of protein synthesis and thus a larger intracellular pool, these data suggest not only that TM- and GPI-AChE are present at similar levels on the cell surface at steady state, but also that they are likely to be delivered there at a similar rate.

DISCUSSION

The data presented here are part of a study designed to explore the roles played by a GPI anchor in the

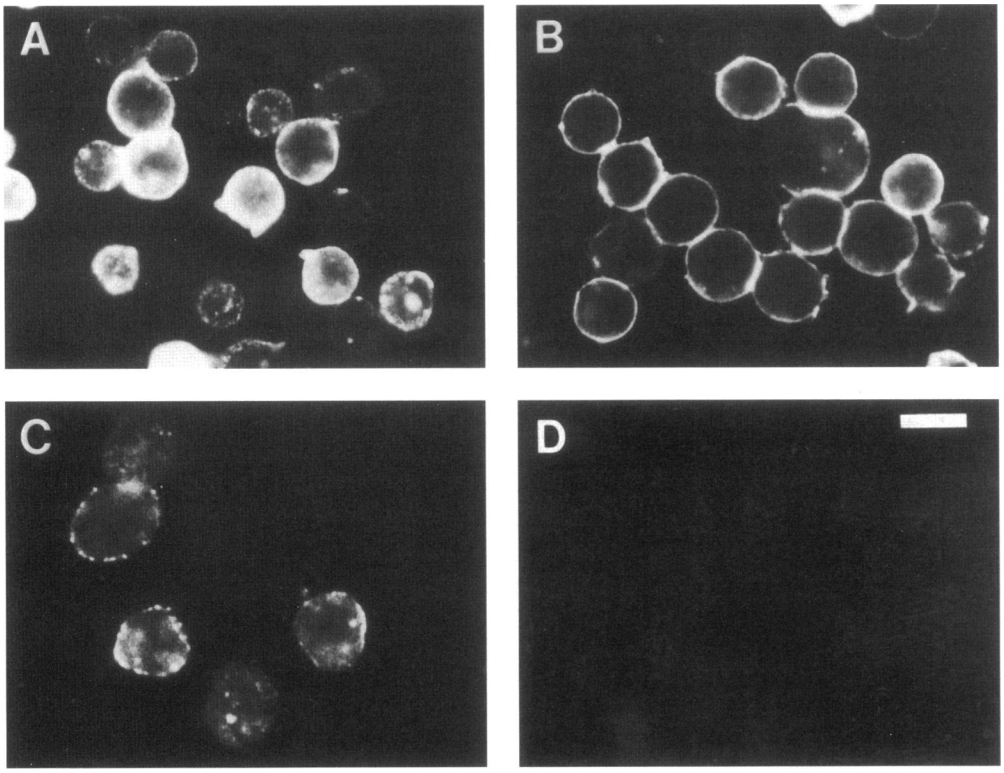

Figure 6. Cell-surface AChE immunocytochemistry on S2 cell lines expressing the four AChE constructs. Cells were attached to poly-L-lysine coated slides, fixed with 4% paraformaldehyde, and labeled with an AChE antiserum and a rhodamine-conjugated secondary antibody as outlined in MATERIALS AND METHODS. (A) E18/3 cells expressing GPI-AChE. (B) GC/8 cells expressing TM-AChE. (C) SEC1/3 cells expressing SEC1. (D) SEC2/4 cells expressing the SEC2. Scale bar, 10 μm.

physiology of a well-understood protein, *Drosophila* AChE. An important goal of the study is the in vivo characterization of any functional consequences that result from the anchoring of AChE by a transmembrane peptide domain rather than by the GPI. To approach this goal we constructed two classes of AChE distinct from the wild-type GPI-anchored form, one involving secreted, nonanchored forms, and the second anchored by the transmembrane domain of HSV-1 gC. The data here demonstrate that these AChE constructs generally have the predicted biochemical and cell biological properties without alteration of enzymatic function. Furthermore, when expressed in transgenic *Drosophila* devoid of wild-type AChE, the secreted AChE construct failed to rescue flies from their embryonic lethal phenotype (our unpublished results). In contrast, the transmembrane-anchored AChE did rescue but with a slightly higher threshold of AChE activity (Incardona and Rosenberry, 1996). The data in this paper allow the transgenic experiments to be interpreted solely on the basis of differences in the C-terminus of AChE.

The insertion of the synthetic *Nhe*I linker encoding stop codons in three frames into a restriction site within the 3′ end of the *Ace* cDNA gave dual benefits: a truncation of the C-terminal signal peptide resulting in SEC1, and the introduction of a unique site for the in-frame insertion of restriction fragments encoding stable transmembrane domains. The most important criterion in choosing an appropriate transmembrane domain was to retain the membrane attachment property of a GPI anchor without introducing extraneous cell signaling elements. Since in most cases GPI-anchored proteins are apically targeted in polarized epithelia, we did not want to add any sequence that is known to confer a basolateral orientation. Because GPI-anchored proteins are bound only to the outer leaflet of the bilayer and thus limited in their direct interactions with intracellular structures, we also sought a transmembrane domain that would not specifically enter coated pits or have other known intracellular interactions. These considerations, in general, require a transmembrane domain without a large cytoplasmic tail. A final criterion was that the transmembrane domain be well characterized, i.e., demonstrated to be membrane bound by truncation or proteolysis studies. All of these criteria appear to be satisfied by the transmembrane domains of several mammalian viral glycoproteins. The first transmembrane domain that we evaluated was that of a truncated version of VSV G. This well-studied domain has been used to anchor chimeric proteins in several reports on the biogenesis and sorting of membrane proteins (eg. Guan *et al.*, 1985; Brown *et al.*, 1989). Although VSV G is basolaterally targeted, an intact cytoplasmic domain and in particular a critical tyrosine residue therein are necessary for this localization (Thomas *et al.*, 1993). We therefore chose a trun-

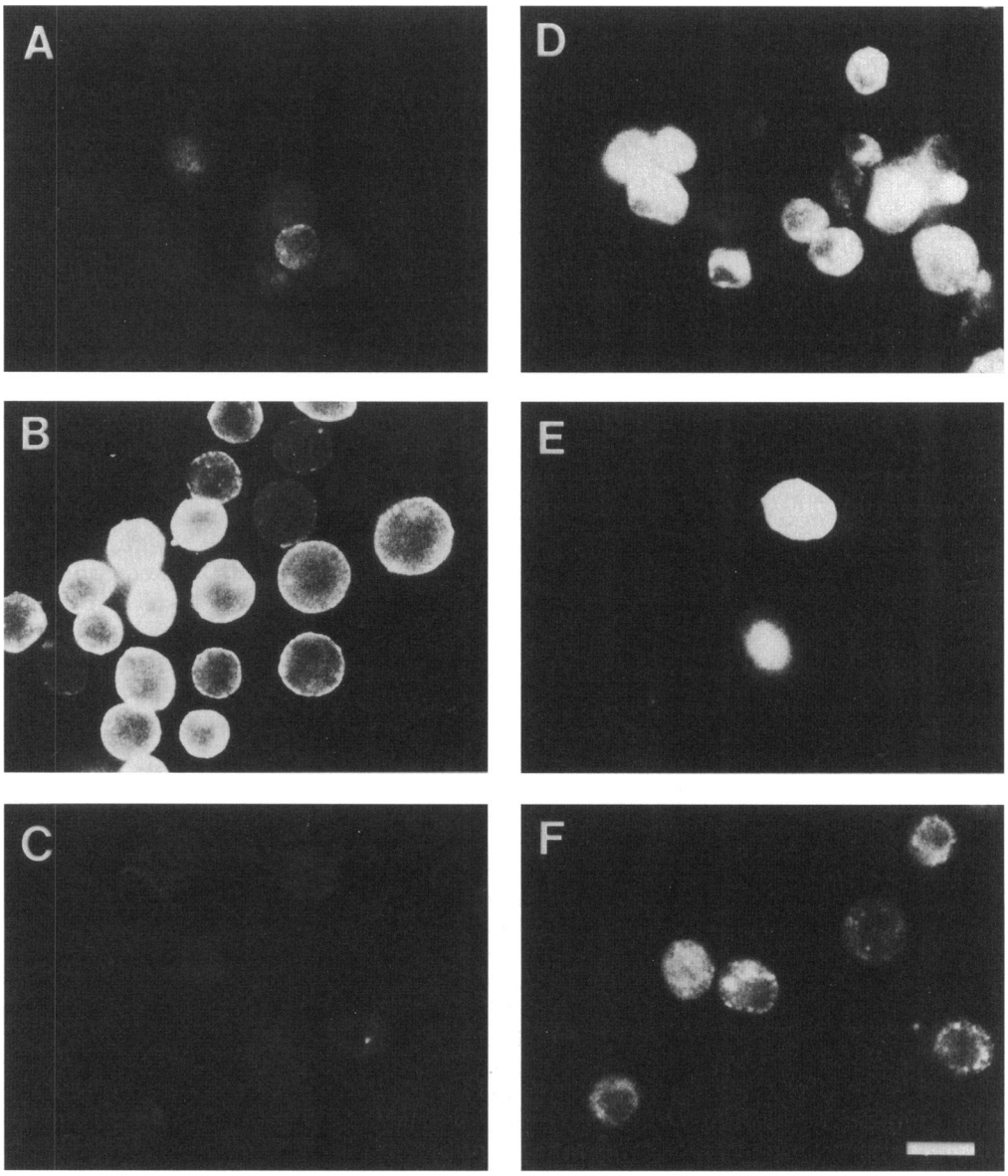

Figure 7. Immunofluorescence of PIPLC-treated S2 lines. The same cell lines shown in Figure 6 were treated with 40 μg/ml PIPLC followed by fixation and immunolabeling as described in Figure 6 and MATERIALS AND METHODS. E18/3, GC/8, or SEC1/3 cells, respectively, before (A–C) or after (D–F) permeabilization with 0.4 mg/ml saponin. Pre-immune serum produced weak background staining with no apparent pattern in permeabilized cells and no background on nonpermeabilized cells (our unpublished observations). Scale bar, 10 μm.

cation mutant CT-3 (Whitt *et al.*, 1989) with only three membrane proximal residues of the cytoplasmic domain, one of which is charged. However, when the CT-3 transmembrane domain/AChE fusion cDNA was transfected into S2 cells, only barely detectable enzyme activity was obtained (our unpublished results). Although this result was not pursued further, we suspect that the G transmembrane domain caused aberrant formation of unstable AChE oligomers.

We subsequently chose a second viral glycoprotein, HSV-1 gC, as a source of a transmembrane domain. HSV-1 gC may exist as a noncovalently associated dimer (Kikuchi *et al.*, 1990), and it has only a small 11-residue cytoplasmic domain with no obvious localization signals. The transmembrane domain has been delineated functionally by a large genetic study of HSV-1 gC negative strains (Homa *et al.*, 1986). Herpes viruses are enveloped at the nuclear membrane (Morgan *et al.*, 1959), and all of the HSV-2 glycoproteins including gC and HSV-1 gD were expressed on the nuclear envelope and on the basolateral surface of several polarized epithelial cell lines (Srivinas *et al.*, 1986). Furthermore, a HSV-1 gC mutant lacking the cytoplasmic tail was still incorporated into virions (Holland *et al.*, 1988), indicating that the cytoplasmic domain at least is not necessary for interaction with capsid or other viral proteins nor is likely to act as a sorting signal. It is unknown if or how any HSV glycoproteins are recycled or internalized by coated pits. We predicted that the HSV-1 gC transmembrane

Table 4. ETP selectively inactivates cell-surface AChE

ETP	PIPLC	In pellet	Supernatant
−	−	100	ND[a]
+	−	24 ± 3	ND
−	+	24 ± 3	66 ± 8
+	+	23 ± 5	7 ± 1

Cells of the line E18/3 expressing GPI-AChE (8×10^7) were pelleted and washed three times with PBS, pH 7.0. After chilling on ice, half were treated with 10 μM ETP in PBS for 30 min on ice. After washing away the ETP with ice-cold PBS, half the treated cells and half the untreated cells were digested with 40 μg/ml PIPLC for 30 min at room temperature. Cells were pelleted and the supernatants saved. After washing the cells twice, triplicate aliquots for all treatments were pelleted in pre-weighed tubes, weighed, and lysed in a volume of DSS buffer equal to five times the pellet weight. Lysates and supernatants of the PIPLC reaction were assayed for AChE activity. Values are expressed as percentages of total activity in the pellet of untreated cells (0.42 ± 0.05 U AChE/mg wet cells) and are the means and standard error of three determinations.

[a] ND, not determined.

domain should be neutral and when fused to the AChE ectodomain produce a PIPLC-resistant membrane-bound protein that is able to dimerize and be processed normally. The ND-PAGE profile (Figure 2), hydrodynamic properties, and SDS-PAGE profile (Figure 5) of the transmembrane AChE chimera expressed in S2 cells are consistent with this prediction. Moreover, PIPLC had no effect on TM-AChE as assessed by four methods (Figures 2 and 7; Tables 2 and 3). The catalytic activity and cellular processing of TM-AChE appeared unaltered from those of the wild type. Additionally, TM-AChE was expressed on the cell surface as assessed by indirect immunofluorescence (Figure 6) with a pattern essentially identical to that of GPI-AChE. A selective assay of intracellular AChE by inactivation of extracellular enzyme with ETP (Table 4) showed that the cell-surface pool is comparable for TM-AChE and GPI-AChE. Therefore, the HSV-1 gC transmembrane and cytoplasmic domains do not interfere with delivery of AChE to the surface and, since the steady state cell-surface pools are equivalent, TM-AChE probably does not have a higher turnover rate than GPI-AChE. Except for a slight difference in binding to Triton X-114, which is probably irrelevant to cellular function, the transmembrane version of AChE that we produced behaved very similarly to the GPI-anchored form. One study has shown that conversion of influenza hemagglutinin from a transmembrane protein to a GPI-anchored form resulted in an alteration in structure distant from the membrane-binding domain with a subsequent decrease in the interaction with ligand (Kemble *et al.*, 1993). Our data on TM-AChE shows no demonstrable alterations in the structure nor function of the AChE catalytic domain.

To construct secreted AChEs, truncations were introduced at two sites near the C-terminal sequence that signals GPI anchoring. SEC1 was generated by removing 25 amino acids at the C-terminus of the native AChE translation product, leaving a short sequence of at most nine residues beyond the Cys^{615} residue retained in the mature dimer. Surprisingly, this remaining C-terminus was still recognized, albeit poorly, as a GPI addition site. As shown qualitatively in Figure 3A and quantitatively in Figure 4, about 4–7.5% of the total AChE produced over a 6-h period by an S2 cell line expressing SEC1 became GPI anchored. Because most of SEC1 was efficiently secreted, a slightly higher proportion (12%) of cell-associated SEC1 was GPI-anchored in the steady state. Truncation of 29 C-terminal residues produced SEC2, with a C-terminal sequence of only five residues beyond Cys^{615}, and the signal for GPI addition was completely eliminated (Figure 3B). Both SEC1 and SEC2 remained disulfide-linked dimers, as shown by the ND-PAGE and SDS-PAGE profiles, and the catalytic activity was not altered. All previous studies of the signals for GPI addition have led to the conclusion that a hydrophobic C-terminal sequence of appropriate length is crucial for attachment of the anchor. Typically, truncations that are less extensive than that in SEC1 resulted in no anchor attachment. For example, the following truncations all were reported to eliminate GPI attachment to the respective proteins: 10 residues of the 30 beyond the mature C-terminus for placental alkaline phosphatase (Berger *et al.*, 1988); 17 of 37 for DAF (Caras *et al.*, 1989); and 12 of 29 for Ly-6E (Su and Bothwell, 1989). There is no precedent for partial GPI addition after such a large truncation as that which produced SEC1. The addition site cannot have been shifted further N-terminally, as the GPI-anchored SEC1 is still dimeric and therefore must still contain Cys^{615}. Contamination of the SEC1 cell lines by wild-type cDNA is unlikely: the phenomenon is seen both in transiently transfected S2 cells (our unpublished observations) and in stable lines transfected with two different preparations of DNA, and it involves all cells in the stable lines (Figure 6C). Furthermore, a similar observation was made in transgenic *Drosophila* expressing SEC1 from an *Ace* minigene construct into which the mutation had been introduced by a separate set of ligations (our unpublished data). Readthrough of the stop codon is a possibility that we are unable to rule out without further experimentation. However, several lines of indirect evidence suggest that this rare event is highly unlikely. There are two documented mechanisms for readthrough of UAG codons. In tobacco mosaic virus readthrough requires a minimal sequence of UAG-CAR-YYA and the Moloney murine leukemia virus *gag-pol* readthrough depends on the formation of a psuedoknot immediately downstream of the UAG codon (reviewed by Weiss, 1991). Exami-

nation of the sequence surrounding the UAG codon of SEC1 AChE shows no consensus sequence and folding of the RNA (Jaeger *et al.*, 1989) from −20 to +100 around the stop codon shows no pseudoknot. Two cases of presumptive readthrough of nonsense mutations have been identified in human lysosomal storage disorders (Yang *et al.*, 1992; Peltola *et al.*, 1994). In these cases, however, readthrough was inferred by the presence of small amounts of full-length inactive protein, and neither involved a UAG codon. Different mechanisms are involved in the readthrough of UAA and UGA codons and are not relevent to our situation. Furthermore, the large majority of readthrough events occur in either viral or transposable element products, or in genetic disorders, all of which involve selective pressure.

SEC1 and SEC2 were efficiently secreted by S2 cell lines and accumulated to high levels in the culture medium (Figure 3, A and B; Figure 4). However, both of these AChEs showed hydrophilic, endo H-sensitive bands associated with a cellular compartment on ND-PAGE gels (Figure 3B). This observation, along with the finding that the hydrophilic component of cell-associated SEC1 approaches its steady-state level more slowly than the GPI-anchored component after MSF treatment (Figure 4), suggests that the secretory pathway for these AChEs may differ from the route by which membrane-bound AChEs reach the cell surface. For example, this difference may reflect the filling of some type of secretory storage vesicle. Although S2 cells are largely uncharacterized biologically, there is circumstantial evidence that they are derived from macrophage-like hemocytes (Abrams *et al.*, 1992). The fact that the truncated AChEs are so readily secreted indicates that the GPI anchor is not necessary for transport out of the endoplasmic reticulum and through the Golgi complex; the AChE ectodomain probably contains all the necessary information for getting to the cell surface. This interpretation is strengthened further by the observation that TM-AChE also appeared unaltered in its delivery to the cell surface.

The biochemical data presented here demonstrate that we have constructed two classes of *Drosophila* AChE with altered or deleted membrane anchoring domains whose catalytic properties do not differ from those of wild-type GPI-AChE. Analysis of the expression patterns of these proteins in S2 cells by both morphological and pharmacological methods shows no gross changes in their processing. No conclusions about a GPI sorting function can be made from these data as S2 cells are unpolarized, and we have not found any evidence for cold Triton-insoluble complexes in these cells. However, GPI-AChE and TM-AChE are sorted identically in polarized epithelial cells of transgenic flies (Incardona and Rosenberry, 1996), indicating that the GPI anchor does not serve as a targeting signal for AChE in *Drosophila*.

ACKNOWLEDGMENTS

We thank Didier Fournier for providing the *Ace* cDNA subclone pE18, Lucy Cherbas for providing the S2 cells and medium recipes, Mark Krasnow for the expression vector pP_{ac}, John K. Rose for the gift of the VSV G CT3 construct, Tom Holland for the HSV-1 gC cDNA, Bill Sugden for the *hph* coding sequence, Pat Thomas for the purification of GPI-AChE from Sf9 cells and production of PIPLC, Jean Eastman for excellent technical assistance and for purifying SEC1, Steve Younkin for suggesting the echothiophate experiment, and Mike LaFontaine of Wyeth-Ayerst Labs for donating the echothiophate. We thank Robert Haas for a thorough critique of the manuscript. This work was supported by grant NS-16577 to T.L.R. from the National Institutes of Health, by grants from the Muscular Dystrophy Association, and by a Medical Scientist Training Program predoctoral fellowship (grant GM-07250) to J.P.I. from the National Institute of General Medical Sciences.

REFERENCES

Abrams, J.M., Lux, A., Steller, H., and Krieger, M. (1992). Macrophages in *Drosophila* and L2 cells exhibit scavenger receptor-mediated endocytosis. Proc. Natl. Acad. Sci. USA *89*, 10375–10379.

Anderson, R.G.W. (1993). Plasmalemmal caveolae and GPI-anchored membrane proteins. Curr. Opin. Cell Biol. *5*, 647–652.

Ashburner, M. (1989). *Drosophila*: A Laboratory Manual, Cold Spring Harbor, NY: Cold Spring Harbor Laboratory Press, 143–145.

Berger, J., Howar, A.D., Brink, L., Gerber, L., Hauber, J., Cullen, B.R., and Udenfriend, S. (1988). COOH-terminal requirements for the correct processing of a phosphatidylinositol-glycan–anchored membrane protein. J. Biol. Chem. *263*, 10016–10021.

Berger, J., Micanovic, R., Greenspan, R.J., and Udenfriend, S. (1989). Conversion of placental alkaline phosphatase from a phosphatidylinositol-glycan–anchored protein to an integral transmembrane protein. Proc. Natl. Acad. Sci. USA *86*, 1457–1460.

Bordier, C. (1988). Analytical and preparative phase separation of glycolipid-anchored membrane proteins in Triton X-114 solution. In: Post-translational Modification of Proteins by Lipids, ed. U. Brodbeck and C. Bordier, Berlin, Germany: Springer-Verlag.

Brockman, S.K., Przybylski, R.J., and Younkin, S.G. (1982). Cellular localization of the molecular forms of acetylcholinesterase in cultured embryonic rat myotubes. J. Neurosci. *2*, 1775–1785.

Brown, D.A., Crise, B., and Rose, J.K. (1989). Mechanism of membrane anchoring affects polarized expression of two proteins in MDCK cells. Science *245*, 1499–1501.

Brown, D.A., and Rose, J.K. (1992). Sorting of GPI-anchored proteins to glycolipid-enriched membrane subdomains during transport to the apical cell surface. Cell *68*, 533–544.

Butters, T.D., Hughes, R.C., and Vischer, P. (1981). Steps in the biosynthesis of mosquito cell membrane glycoproteins and the effects of tunicamycin. Biochim. Biophys. Acta *640*, 672–686.

Caras, I.W., Weddell, G.N., and Williams, S.R. (1989). Analysis of the signal for attachment of a glycophospholipid membrane anchor. J. Cell Biol. *108*, 1387–1396.

Cinek, T., and Hořejší, V. (1992). The nature of large noncovalent complexes containing glycosyl-phosphatidylinositol–anchored membrane glycoproteins and protein tyrosine kinases. J. Immunol. *149*, 2262–2270.

Crise, B., Ruusala, A., Zagouras, P., Shaw, A., and Rose, J.K. (1989). Oligomerization of glycolipid-anchored and soluble forms of the vesicular stomatitis virus glycoprotein. J. Virol. *63*, 5328–5333.

Davitz, M.A., Hom, J., and Schenkman, S. (1989). Purification of a glycosyl-phosphatidylinositol–specific phospholipase D from human plasma. J. Biol. Chem. *264*, 13760–13764.

Deeg, M.A., Humphrey, D.R., Yang, S.H., Ferguson, T.R., Reinhold, V.N., and Rosenberry, T.L. (1992). Glycan components in the glycoinositol phospholipid anchor of human erythrocyte acetylcholinesterase. J. Biol. Chem. *267*, 18573–18580.

Dotti, C.G., Parton, R.G., and Simons, K. (1991). Polarized sorting of glypiated proteins in hippocampal neurons. Nature *349*, 158–161.

Dupree, P., Parton, R.G., Raposo, G., Kurzchalia, T.V., and Simons, K. (1993). Caveolae and sorting in the *trans*-Golgi network of epithelial cells. EMBO J. *12*, 1597–1605.

Ellman, G.L., Courtney, K.D., Andress, V., and Featherstone, R.H. (1961). A new and rapid colorimetric determination of acetylcholinesterase activity. Biochem. Pharmacol. *7*, 88–95.

Englund, P.T. (1993). The structure and biosynthesis of glycosyl phophatidylinositol protein anchors. Annu. Rev. Biochem. *62*, 121–138.

Fox, J.A., Soliz, N.M., and Saltiel, A.R. (1987). Purification of a phosphatidylinositol-glycan–specific phospholipase C from liver plasma membranes: a possible target of insulin action. Proc. Natl. Acad. Sci. USA *84*, 2663–2667.

Frink, R.J., Eisenberg, R., Cohen, G., and Wagner, E.K. (1983). Detailed analysis of the portion of the herpes simplex virus type 1 genome encoding glycoprotein C. J. Virol. *45*, 634–647.

Gnagey, A.L., Forte, M., and Rosenberry, T.L. (1987). Isolation and characterization of acetylcholinesterase from *Drosophila*. J. Biol. Chem. *262*, 13290–13298.

Gritz, L., and Davies, J. (1983). Plasmid-encoded hygromycin B resistance: the sequence of hygromycin B phosphotransferase gene and its expression in *Escherichia coli* and *Saccharomyces cerevisiae*. Gene *25*, 179–188.

Guan, J.-L., Machamer, C.E., and Rose, J.K. (1985). Glycosylation allows cell-surface transport of an anchored secretory protein. Cell *42*, 489–496.

Hall, L.M.C., and Spierer, P. (1986). The *Ace* locus of *Drosophila melanogaster*: structural gene for acetylcholinesterase with an unusually long 5′ leader. EMBO J. *5*, 2949–2954.

Herald, D., Krakow, J.L., Bangs, J.D., Hart, G.W., and Englund, P.T. (1986). A phospholipase C from *Trypanosoma brucei* which selectively cleaves the glycolipid on the variant surface glycoprotein. J. Biol. Chem. *261*, 13813–13819.

Hoener, M.C., Stieger, S., and Brodbeck, U. (1990). Isolation and characterisation of a phosphatidylinositol-glycan-anchor–specific phopholipase D from bovine brain. Eur. J. Biochem. *190*, 593–601.

Holland, T.C., Lerch, R.J., and Earhart, K. (1988). The cytoplasmic domain of herpes simplex virus type 1 glycoprotein C is required for membrane anchoring. J. Virol. *62*, 1753–1761.

Homa, F.L., Purifoy, D.J.M., Glorioso, J.C., and Levine, M. (1986). Molecular basis of the glycoprotein C-negative phenotypes of herpes simplex virus type 1 mutants selected with a virus-neutralizing monoclonal antibody. J. Virol. *58*, 281–289.

Hsieh, P., and Robbins, P.W. (1984). Regulation of asparagine-linked oligosaccharide processing. J. Biol. Chem. *259*, 2375–2382.

Incardona, J.P., and Rosenberry, T.L. (1996). Replacement of the glycoinositol phospholipid anchor of *Drosophila* acetylcholinesterase with a transmembrane domain does not alter sorting in neurons and epithelia but results in behavioral defects. Mol. Biol. Cell. *7*, 613–630.

Jaeger, J.A., Turner, D.H., and Zuker, M. (1989). Improved predictions of secondary structures for RNA. Proc. Natl. Acad. Sci. USA *86*, 7706–7710.

Karnovsky, M.J., and Roots, L. (1964). A "direct-coloring" thiocholine method for cholinesterases. J. Histochem. Cytochem. *12*, 219–222.

Kemble, G.W., Henis, Y.I., and White, J.M. (1993). GPI- and transmembrane-anchored influenza hemagglutinin differ in structure and receptor binding activity. J. Cell Biol. *122*, 1253–1265.

Kikuchi, G.E., Glorioso, J.C., and Nairn, R. (1990). Cross-linking studies show that herpes simplex virus type I glycoprotein C molecules are clustered in the membrane of infected cells. J. Gen. Virol. *71*, 455–458.

Krasnow, M.A., Saffman, E.E., Korenfeld, K., and Hogness, D.S. (1989). Transcriptional activation and repression by *Ultrabithorax* proteins in cultured *Drosophila* cells. Cell *57*, 1031–1043.

Kuroda, K., Geyer, H., Geyer, R., Doerfler, W., and Klenk, H.-D. (1990). The oligosaccharides of influenza virus hemagglutinin expressed in insect cells by a baculovirus vector. Virology *174*, 418–429.

Laemmli, U.K. (1970). Cleavage of structural proteins during the assembly of the head of bacteriophage T4. Nature *227*, 680–685.

Lisanti, M.P., Caras, I.W., Davitz, M.A., and Rodriguez-Boulan, E. (1989). A glycophospholipid membrane anchor acts as an apical targeting signal in polarized epithelial cells. J. Cell. Biol. *109*, 2145–2156.

Low, M.G., and Prasad, A.R.S. (1988). A phospholipase D specific for the phosphatidylinositol anchor of cell-surface proteins is abundant in plasma. Proc. Natl. Acad. Sci. USA *85*, 980–984.

Morgan, C., Holden, M., and Jones, E.P. (1959). Electron microscopic observations on the development of herpes simplex virus. J. Exp. Med. *110*, 643–656.

Mutero, A., and Fournier, D. (1992). Post-translational modifications of *Drosophila* acetylcholinesterase. J. Biol. Chem. *267*, 1695–1700.

Peltola, M., Chiatayat, D., Peltonen, L., and Jalanko, A. (1994). Characterization of a point mutation in aspartylglucosaminidase gene: evidence for a readthrough of a translational stop codon. Hum. Mol. Genet. *3*, 2237–2242.

Restifo, L.L., and White, K. (1990). Molecular and genetic approaches to neurotransmitter and neuromodulator systems in *Drosophila*. Adv. Insect Physiol. *22*, 115–219.

Robinson, P.J. (1991). Phosphatidylinositol membrane anchors and T-cell activation. Immunol. Today *12*, 35–41.

Robinson, P.J., Millrain, M., Antoniou, J., Simpson, E., and Mellor, A.L. (1989). A glycophospholipid anchor is required for Qa-2-mediated T cell activation. Nature *342*, 85–87.

Rosenberry, T.L., and Scoggin, D.M. (1984). Structure of human erythrocyte acetylcholinesterase. J. Biol. Chem. *259*, 5643–5652.

Rotundo, R.L. (1988). Biogenesis of acetylcholinesterase molecular forms in muscle. J. Biol. Chem. *263*, 19398–19406.

Sargiacomo, M., Sudol, M., Tang, Z.L., and Lisanti, M.P. (1993). Signal transducing molecules and glycosyl-phosphatidylinositol–

linked proteins form a caveolin-rich insoluble complex in MDCK cells. J. Cell Biol. *122*, 789–807.

Shields, D., and Sang, J.H. (1977). Improved medium for culture of *Drosophila* embryonic cells. Drosophila Inf. Service *52*, 161.

Srivinas, R.V., Balachandran, N., Alonso-Caplen, F.V., and Compans, R.W. (1986). Expression of herpes simplex virus glycoproteins in polarized epithelial cells. J. Virol. *58*, 689–693.

Štefanová, I., Hořejší, V., Ansotegui, I.J., Knapp, W., and Stockinger, H. (1991). GPI-anchored cell-surface molecules complexed to protein tyrosine kinases. Science *254*, 1016–1019.

Su, B., and Bothwell, A.L.M. (1989). Biosynthesis of a phosphatidylinositol-glycan–linked membrane protein: signals for posttranslational processing of the Ly-6E antigen. Mol. Cell. Biol. *9*, 3369–3376.

Tago, H., Kimura, H., and Maeda, T. (1986). Visualization of detailed acetylcholinesterase fiber and neuron staining in rat brain by a sensitive histochemical procedure. J. Histochem. Cytochem. *34*, 1431–1438.

Thomas, D.C., Brewer, C.B., and Roth, M.G. (1993). Vesicular stomatitis virus glycoprotein contains a dominant cytoplasmic basolateral sorting signal critically dependent on a tyrosine. J. Biol. Chem. *268*, 3313–3320.

Thomas, P.M., and Samelson, L.E. (1992). The glycophosphatidylinositol-anchored Thy-1 molecule interacts with the $p60^{fyn}$ protein tyrosine kinase in T cells. J. Biol. Chem. *267*, 12317–12322.

Toutant, J.-P., Richards, M.K., Krall, J.A., and Rosenberry, T.L. (1990). Molecular forms of acetylcholinesterase in two sublines of human erythroleukemia K562 cells. Eur. J. Biochem. *187*, 31–38.

Vigny, M., Bon, S., Massoulie, J., and Gisiger, V. (1979). The subunit structure of mammalian acetylcholinesterase: catalytic subunits, dissociating effects of proteolysis and disulfide reduction of the polymeric forms. J. Neurochem. *33*, 559–565.

Vigny, M., Bon, S., Massoulie, J., and Leterrier, F. (1978). Active-site catalytic efficiency of acetylcholinesterase molecular forms in *Electrophorus*, *Torpedo*, rat and chicken. Eur. J. Biochem. *85*, 317–323.

Weiss, R.B. (1991). Ribosomal frameshifting, jumping and readthrough. Curr. Opin. Cell Biol. *3*, 1051–1055.

Whitt, M.A., Chong, L., and Rose, J.K. (1989). Glycoprotein cytoplasmic domain sequences required for rescue of vesicular stomatitis virus glycoprotein mutant. J. Virol. *63*, 3569–3578.

Yang, M., Allen, H., and DiCoccio, R.A. (1992). A mutation generating a stop codon in the α-L-fucosidase gene of a fucosidosis patient. Biochem. Biophys. Res. Commun. *189*, 1063–1068.

Younkin, S.G., Rosenstein, C., Collins, P.L., and Rosenberry, T.L. (1982). Cellular localization of the molecular forms of acetylcholinesterase in rat diaphragm. J. Biol. Chem. *257*, 13630–13637.